Available online at www.CivileJournal.org

Civil Engineering Journal

(E-ISSN: 2476-3055; ISSN: 2676-6957)

Vol. 8, No. 02, February, 2022

Effect of Pumice Stone and Sugar Molasses on the Behavior of Reinforced Concrete One-Way Ribbed Slabs

Tamara Amer Mohammed [1*], Hayder Mohammed Kadhim [1]

[1] *Civil Engineering Department, College of Engineering, University of Babylon, Babylon, 51001, Iraq.*

Received 01 November 2021; Revised 09 January 2022; Accepted 17 January 2022; Published 01 February 2022

Abstract

The world is currently heading towards sustainability by reducing the amount of concrete, thus reducing the total unit weight. Moreover, design construction requires materials with a higher strength-to-weight ratio. Ribbed slabs and lightweight concrete (LWC) are considered two leading sustainability facilities. This research developed an experimental study to evaluate the effects of concrete type, steel reinforcement ratio, the geometry of ribs, voiding ratio, and slab type on the structural behavior of one-way ribbed slabs. Eight of the one-way slabs were constructed using pumice stone and by-product material sugar molasses (SM), and one slab was constructed using gravel and SM. These slabs were tested under a static two-point load and simply supported until failure. The results showed that using SM with pumice stone instead of gravel led to high strength-lightweight concrete (HSLWC), with a cylinder compressive strength of 42.2 MPa and a density of 1943 kg/m^3, which meets the requirements of HSLWC codes. Using HSLWC instead of high-strength normal-weight concrete (HSNWC) decreased the thermal conductivity by 43.55% and the unit weight by 19.31%. Moreover, the ultimate strength of the HSLWC one-way ribbed slab decreased by 17.70%. Overcoming this strength reduction necessitated increasing the steel reinforcement ratio of the ribs from 0.28 to 0.44% in the HSLWC ribbed slab. Changing the number of ribs at the same amount of HSLWC showed a minor effect on the strength capacity of slabs but showed an economic benefit. However, increasing the rib width to reduce the voiding ratio from 44 to 40% resulted in a greater improvement in structural efficiency (SE) of one-way ribbed slab than reducing it from 44 to 33%. Consequently, the optimum rib width was 120 mm. Moreover, using a ribbed slab instead of a solid slab of HSLWC at the same amount of concrete increased the ultimate strength by 130.37%, decreased deflection by 3.99%, and improved SE by 126.46%. Furthermore, experimental results of ultimate load were compared with the ACI 318-19 code design equation.

Keywords: Ribbed Slab; Pumice Stone; Sugar Molasses; High Strength-Lightweight Concrete; Solid Slab.

1. Introduction

The self-weight of the slab is considered the most significant proportion of the superstructure weight of multi-story buildings. For this reason, the reduction of slab weight is an efficient issue, especially with long-span members and high-rise (multi-story) buildings [1]. This reduction in weight contributes to sustainable construction by using less concrete. Two approaches may be used to reduce slab weight: the first is the (geometric effect), which is tackled using different slabs such as a one-way ribbed slab (joist slab) system. This system consists of regularly spaced concrete joists or ribs spanning in one direction. A reinforced concrete slab was cast integrally with ribs and beam span between the columns perpendicular to the ribs. The weight reduction is achieved by removing the part of the concrete volume

* Corresponding author: eng.tamaraamer@gmail.com

http://dx.doi.org/10.28991/CEJ-2022-08-02-011

underneath the neutral axis of the typical solid slab. Also, high-strength concrete (HSC) provides a better solution for reducing the size and weight of concrete structural elements [2]. The second is (material effect) using lightweight concrete (LWC). Using waste material in concrete production, which has a detrimental effect on the environment, is considered another perspective on sustainably. As a result, sugar molasses, a by-product of sugar cane's viscous refining processes in sugar factories, was used as an admixture in concrete because it acts as a sugar [3].

The effect of lightweight aggregate (LWA) on the behavior of one–way slabs has been studied by many authors; Altun and Haktanir (2001) [4], Adil and Abdul Razzaq (2017) [5], Jomaa'h et al. (2018) [6], Adheem et al. (2018) [7], and Babu and Rex (2019) [8]. However, these studies have often focused on one-way solid slabs and normal-strength concrete (NSC). Khalil (2018) [9] conducted an experimental study that included testing eleven LWA-reinforced concrete slabs with crushed brick as LWA. These slabs have a solid and styropor block slab (SBS) type with different sizes of blocks (percentage of the reduction in weight) and the shear-span to the effective depth ratio (a/d). The use of minimum shear reinforcement and the reduction in the cross-sectional area of SBS resulted in an increase in strength capacity compared to a lightweight solid slab. The wide ribs in SBS perform better than narrow ribs at the same cross-sectional area, and the reduction in (a/d) for LWA solid and styropor block slabs increases the ultimate strength of these slabs.

Al-Nasra et al. (2019) [10] studied the effect of the rib spacing on the performance of the reinforced concrete one-way ribbed slabs. The overall thickness, the design of the concrete mix, and the embedded steel reinforcement were kept constant. Five slabs were prepared and tested by flexural bending stress. The test outcomes showed that the increase in the rib spacing led to a decrease in the slab's strength and a slight decrease in the strength to weight ratio. Vaivade et al. (2019) [11] presented a comparison between high-performance concrete (HPC) and high-performance fiber reinforced concrete (HPFRC) at the ultimate and serviceability limit states of ribbed slabs by using numerical analysis. The variables in this study were the slab height 200 to 340 mm and span length 6 to 12 m. The numerical results showed that using HPFRC instead of HPC increased the intensity of uniformly distributed load by 42 to 46% for ribbed slabs with identical cross-sections and allowable deflections. Also, HPFRC provided a 20% reduction in additional longitudinal reinforcement and cross-section dimensions of the ribbed slab. Huang et al. (2019) [12] conducted experimental work to study the flexural behavior of a large-span multi-ribbed composite slab (R-CS) with filled LWC blocks (autoclaved aerated concrete blocks). The four R-CS specimens and one conventional concrete cast-in-place slab were subjected to static bending testing. According to this study, the R-CS specimens' bending failure process was similar to that of a cast-in-place slab. The deflection, crack development, and ductility were generally good. The ultimate bearing capacity of four R-CS specimens increased by 36.4 to 47.5%, and their unit weight decreased by 17.0 to 30.6% compared with a cast-in-place one.

Liu et al. (2020) [13] An experimental study was carried out to investigate the influence of the three different rib shapes (rectangle, inverted T, and dumbbell) on the flexural behavior of the prestressed concrete composite slab with precast inverted T-shaped ribbed panels (CSPRPs). The test findings showed that the static behaviors of CSPRPs with varied rib shapes, such as cracking load, ultimate bearing capacity, and deflection, were similar. The concrete layers (precast and cast-in-place) can operate together. Abdulhussein and Alfeehan (2020) [14] studied the behavior of normal-strength lightweight reinforced concrete ribbed slabs. The variable in this study was the ratio of the rib depth to the total beam depth. The results revealed that increasing the rib depth to total beam depth ratio enhanced structural behavior by improving load-carrying capacity and lowering deflection. Vaivade et al. (2021) [15] focused on determining the impact of using HPFRC for timber-concrete composite (TCC) ribbed slabs with adhesive connections between layers as the most effective connection type for composite action throughout developing numerical models. Experiment data was used to validate three-dimensional finite element models of timber and ordinary concrete composite ribbed slabs and HPFRC with additional longitudinal reinforcement ribbed slabs. The obtained results demonstrated that replacing the ordinary concrete layer with HPFRC in TTC ribbed slabs with adhesive connection decreased vertical mid-span displacements up to 1.68 times and increased the energy absorption.

There is a lack of available information on the structural behavior of high-strength reinforced concrete one-way ribbed slabs made from normal-weight aggregate (NWA) or LWA together with by-product material such as sugar molasses. This study aims to close the gap in limited information related to the structural behavior of HSC one-way ribbed slabs with T-shape ends and benefit from the characteristics of LWA in improving the unit weight, thermal, and sound insulation of slabs.

2. Experimental Program

Figure 1 shows the experimental program methodology that was adopted in this study.

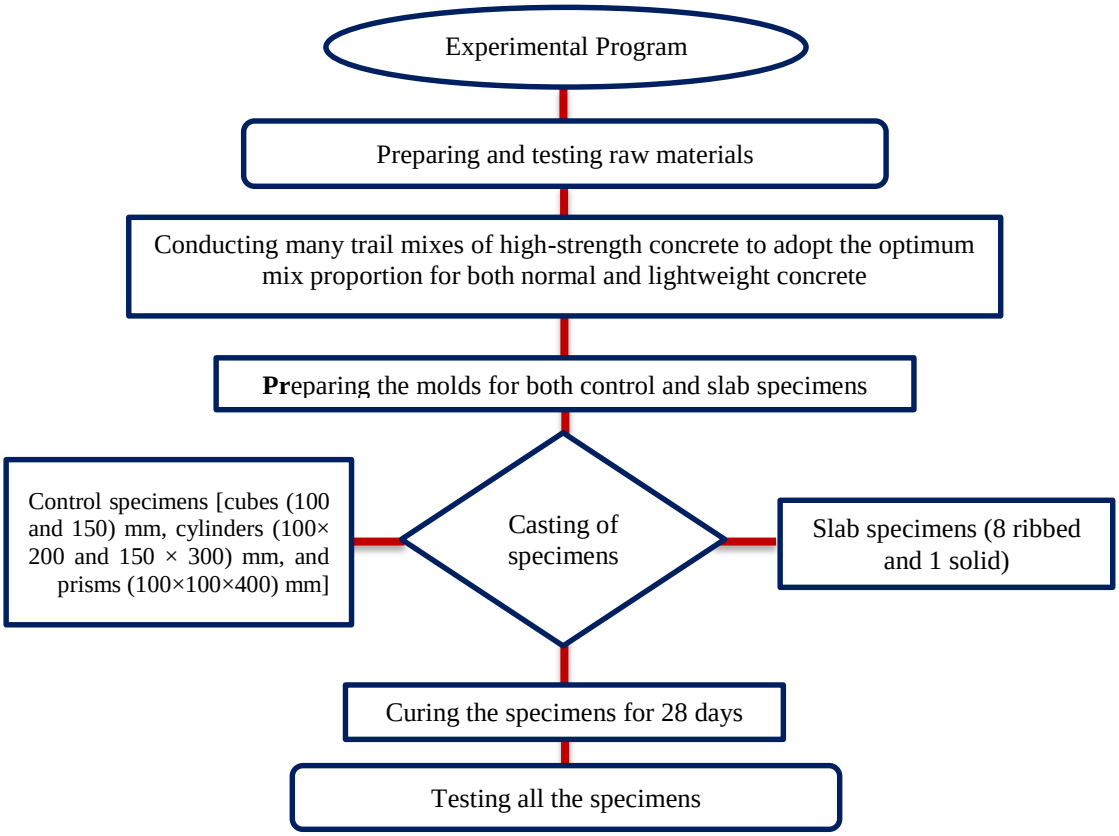

Figure 1. Experimental program methodology

2.1. Details of Specimens and Materials

Details of Specimens

The experimental program included studying the effects of the concrete type, steel reinforcement ratio, geometry section of ribs, voiding ratio, and slab type by testing nine slab specimens as illustrated in Table 1. The program consisted of casting and testing eight reinforced concrete one-way ribbed slabs with dimensions 2000 mm length, 900 mm width, and 150 mm depth. One of these slab specimens was casted with HSNWC, and the others with HSLWC. The last specimen was HSLWC one–way solid slab with a depth of 83mm (to give an equivalent concrete volume of one–way ribbed slab). According to ACI-318-19 [12], the one-way reinforced concrete slab was designed using the ultimate method to fail by flexure mode under the two-point load. All minimum steel reinforcement in the flange and minimum shear reinforcement was the same amount in all one–way ribbed slab specimens. Square mesh reinforcement of (Ø6@150mm c/c in both directions) was used in the flange to meet the shrinkage and temperature reinforcement requirements. To avoid the occurrence of shear failure, (20-Ø6) mm diameter stirrups were provided in each rib. The clear cover at the bottom was 20mm for all slabs. The geometry and steel reinforcement details of the one-way slab sections are shown in Figure 2.

Table 1. Designation and details of the tested slabs

Study Effect of	Slab Symbol	Type of Concrete	Variable	
All Effects	S1	HSLWC	Reference	
Concrete Type	S2	HSNWC	Coarse Aggregate Type	
Steel Reinforcement Ratio	S3	HSLWC	Diameter of Bar	Ø 6 mm
	S4			Ø 10 mm
Geometry of Ribs	S5	HSLWC	Number of Rib	2
	S6			1
Voiding Ratio	S7	HSLWC	Width of Rib	120 mm
	S8			150 mm
Slab Type	S9	HSLWC	Solid Slab	

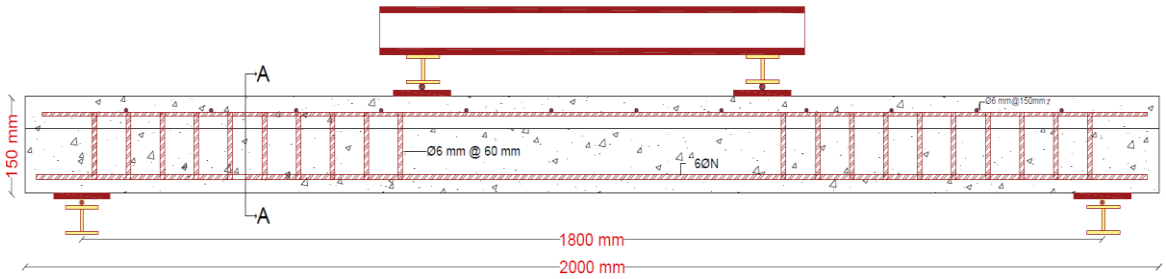

(a) Geometry and reinforcement details for specimens (S1 to S8)

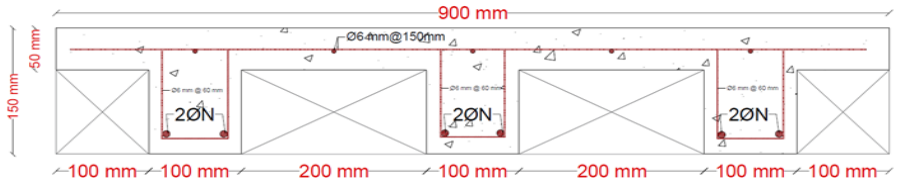

(b) Section A-A for specimens (S1 to S4): Note: N=8 mm for Specimens S1 and S2, N= 6 mm for Specimen S3, N= 10 mm for Specimen S4

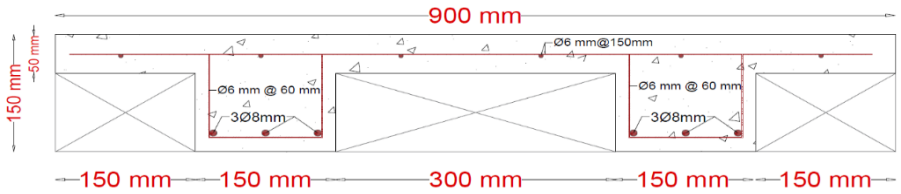

(c) Section A-A for specimen S5

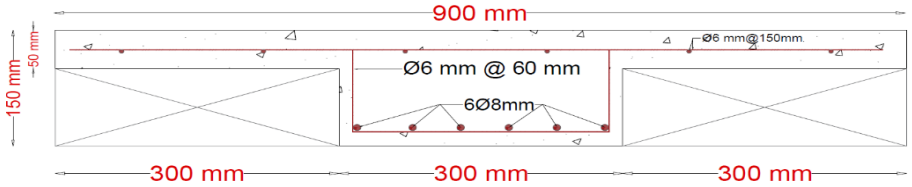

(d) Section A-A for specimen S6

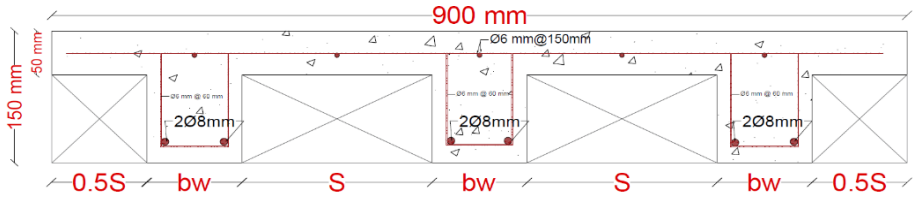

(e) Section A-A for specimens (S7 and S8)- Note: bw= 120mm for Specimen S7, bw= 150mm for Specimen S8

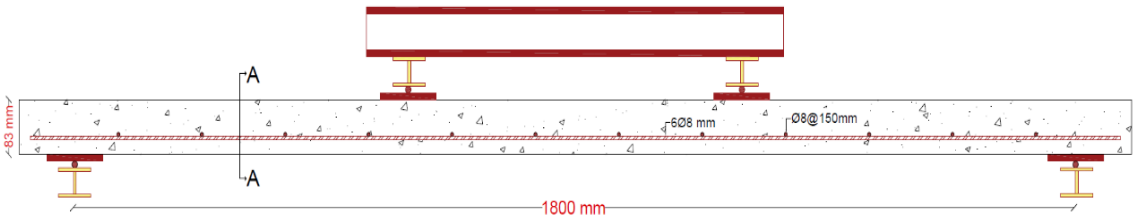

(f) Geometry and reinforcement details for specimen S9

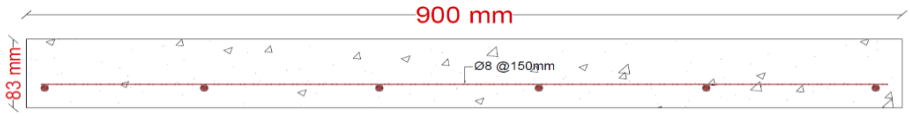

(g) Section A-A for specimen S9

Figure 2. Geometry and reinforcement details of specimens

Properties of Materials

Limestone Portland cement (CEM II/A-L 42.5R) meets with the limitations of EN179-1:2011 [16]. Silica fume, known commercially as MgaAdd MS(D), was used in this study and conformed to ASTM C 1240 [17]. Al-Akaidur fine aggregate (sand) was used in all mixes; the grading curve of this sand conformed to the limitations of Iraqi specification No.45/1984 [18], zone 2, as shown in Figure 3a. Normal-weight coarse aggregate (crushed gravel) with dry density 1570 kg/m^3 was used in the HSNWC mix; the grading curve of this gravel is shown in Figure 3b and conformed to Iraqi specification No.45/1984 [18]. LWA volcanic type (pumice stone) with dry density 708 kg/m^3 was used to produce HSLWC. Figure 3c illustrates the pumice stone grading, which conforms to the ASTM C 330 [19]. High-rang water-reducing admixture, known as ViscoCrete 5930-L, meets the requirement of ASTM C494 [20]; in addition, sugar molasses with a pH 5.37 and Brix 8 [3] added to mixtures to enhance the workability. Finally, tap water was used in all mixes. Table 2 shows the mechanical properties of all deformed steel bars used to reinforce all slab specimens that conform to the ASTM A-650 [21]. Plywood sheets with 20mm thickness were used to fabricate all slab specimens' formworks, as shown in Figure 4.

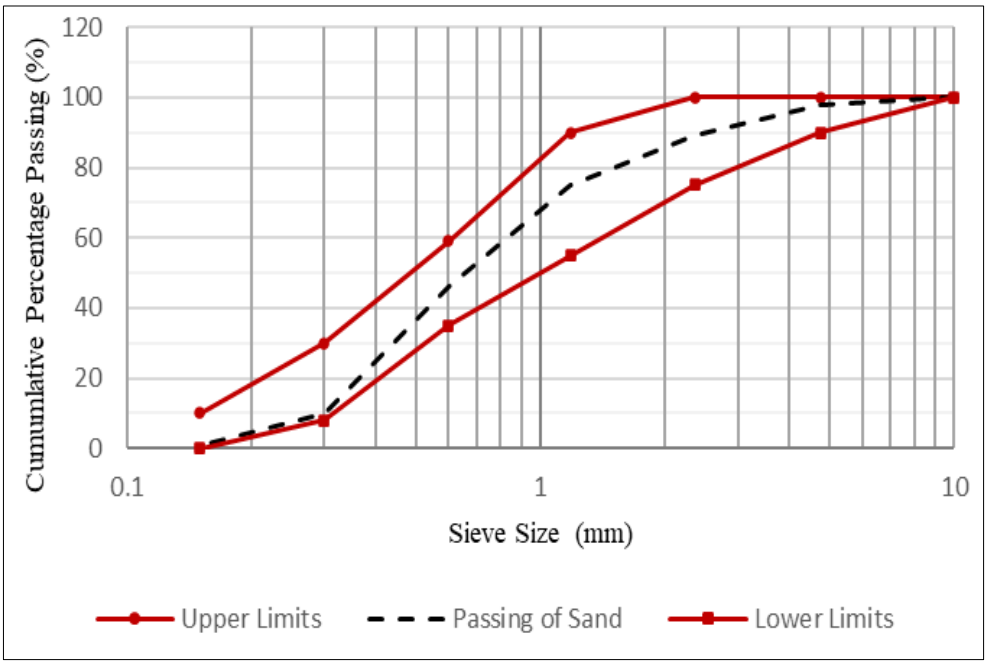

(a) Sieve analysis curve of sand

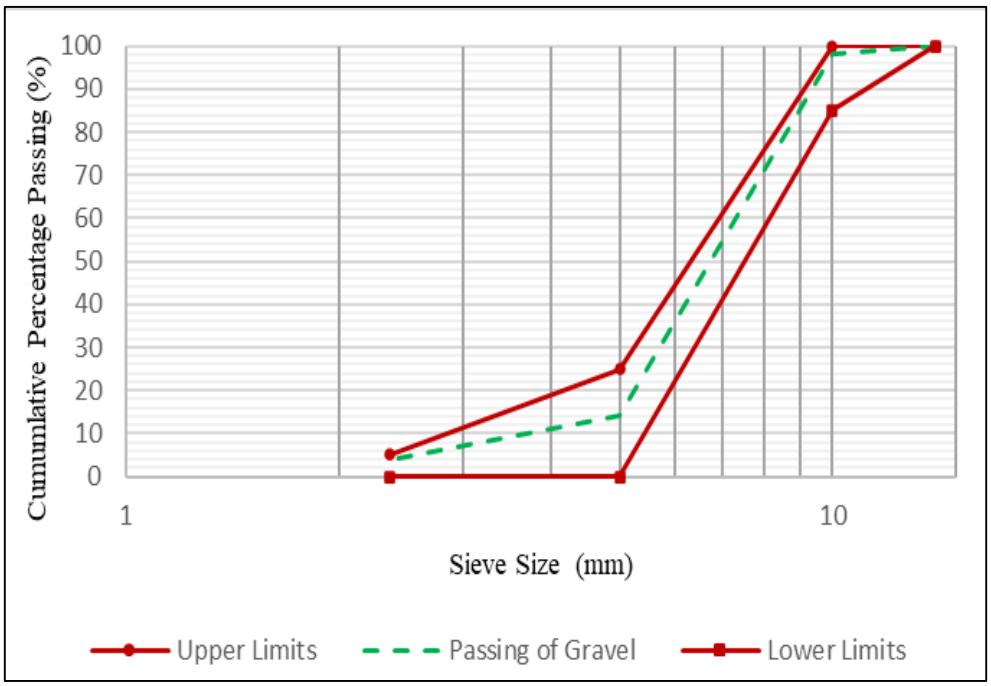

(b) Sieve analysis curve of gravel

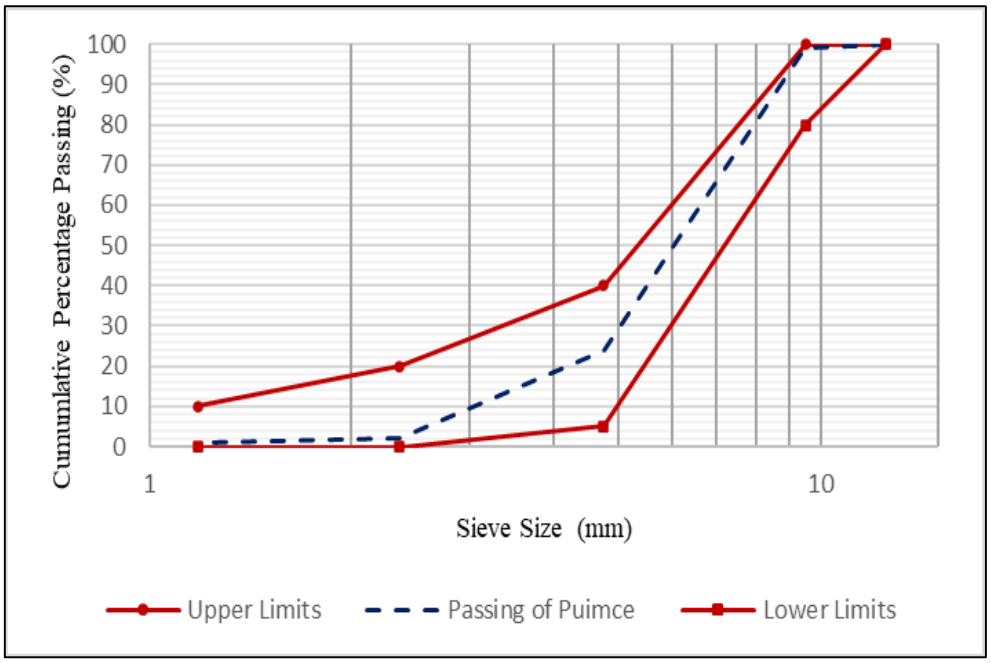

(c) Sieve analysis curve of pumice stone

Figure 3. Grading curves for fine and coarse aggregate

Table 2. Mechanical properties of steel reinforcing bars

Bar Diameter (mm)	Yield Stress (MPa)	Ultimate Stress (MPa)	Elongation %
6	495	541	2
8	509	656	11
10	555	636	8

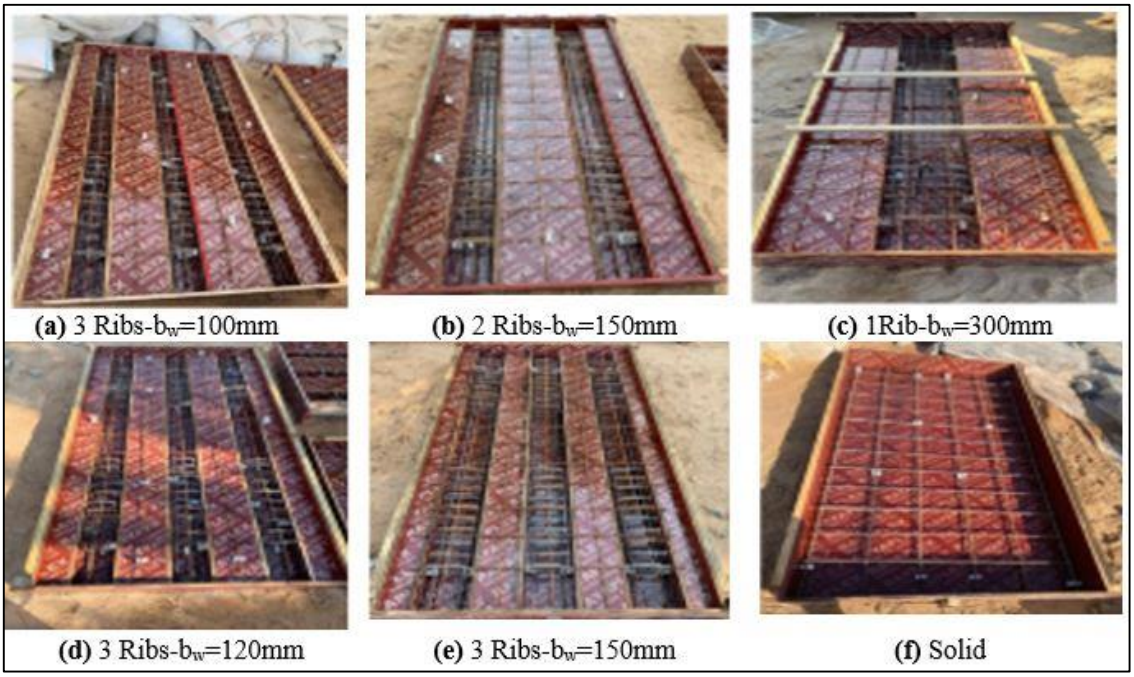

Figure 4. Plywood formworks

Many trail mixes were conducted to choose the optimum concrete mix proportions that meet the required requirements of the ACI 213R-14 [22] for HSLWC and the ACI 363R-10 for HSNWC [23]. Same mix proportions were used in both HSLWC and HSNWC mixes except coarse aggregate type (pumice stone in HSLWC and gravel in HSNWC at same volumetric ratio), as shown in Table 3.

Table 3. Concrete mixes

Materials	Concrete Mixes Quantity (Kg/m^3)	
	HSLWC	HSNWC
Cement	525	525
Silica Fume	75	75
Sand	590	590
Gravel	----	1100
Pumice Stone	495	----
Water	142	142
Superplasticizer	7.85	7.85
Sugar Molasses	1.05	1.05

2.2. Testing Setup

Tests of concrete properties were compressive strength (f_{cu} and f_c`), splitting tensile strength (f_t), modulus of rupture (f_r), ultrasonic pulse velocity (UPV), dry density (w_c), and thermal conductivity (λ) that carried out following (BS 1881-116 [24], ASTM C39 [25]), ASTM C496 [26], ASTM C78 [27], ASTM C597 [28], (ASTM C567 [29] and ASTM C642 [30]), and ASTM C1113 [31], respectively. All slab specimens were tested by a hydraulic jack testing machine of (60 Ton) capacity in the construction laboratory of Civil Engineering College, Babylon University. The control panel of the testing machine contains the hydraulic power unit, the load measuring unit, and the control devices. The load was applied to slabs through a spreader steel beam, which was applied in load control mode.

The supporting condition for all slab specimens was simply supported by using a roller and hinge support. Both hinge and roller support consists of a steel plate with a 20mm thickness and a 10mm steel circular shaft that was welded with I-section. The hinge support was manufactured to limit horizontal displacement while still allowing for rotation, while roller support was manufactured to allow both rotation and horizontal displacement. Steel bearing plates with a 20mm thickness are laid at points of supports and loading to prevent the local crushing. The slab specimen was precisely aligned in the testing machine with locations of loading and support. The effective span for all tested slabs was 1800mm, with a distance between two-point loading (600) mm, as shown in Figure 5. The optical micrometer with 0.02 mm accuracy was used to measure the cracks widths of all slab specimens. The deflection of slab specimens was measured at the mid-span of the slab using LVDT with a maximum capacity of 100 mm (KTR-100mm) with a 0.01mm accuracy. The load cell with (200 Ton) capacity and with precision (24-bit-analog to digital converter (ADC)) was used to measure the applied load. Hx 711 Datalogger amplifier with 12-channel was used to collect the data. It was connected to the Dell Precision M 4800 laptop; this laptop supplied by a particular program was done in LabView 2020 to receive all data and save it as an Excel file. The load was applied in stages at a loading rate of 0.05kN/s. The observations and measurements data of applied load, midspan deflection, crack propagation, and development on the faces and surface of the slab were recorded at each loading interval.

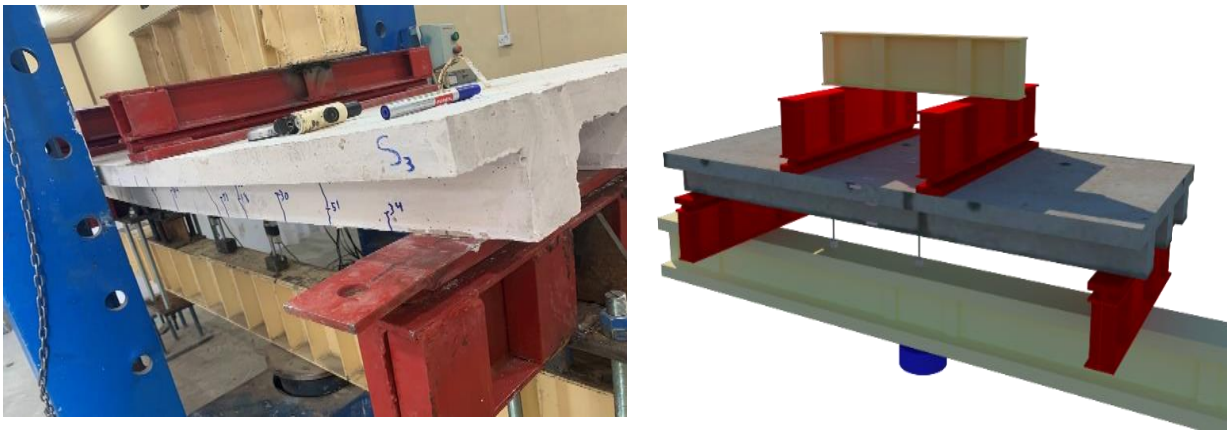

(a) Experimental model (b) Sketchup model

Figure 5. Experimental testing of slab specimen

3. Results and Discussion

3.1. Concrete Properties Results

Tables 4 summarizes the results of mechanical properties for both HSLWC and HSNWC mixes. From these results can be seen that using HSLWC instead of HSNWC decreased f_{cu}, f_c`, f_t, f_r, and UPV by about 23.61, 27.24, 34.04, 37.5,

and 19.06%, respectively, because of the porous nature of LWA that weakens the aggregate. Moreover, using LWA decreased the values of w_c, λ, and AI by about 19.31, 43.55, and 34.85%, respectively.

Table 4. Mechanical properties of concrete mixes*

Concrete Mix	f_{cu} (MPa)	f_c` (MPa)	f_t (MPa)	f_r (MPa)	UPV (km/s)	w_c (kg/m^3)	λ** W/ (m.K)	AI*** Rayl
HSLWC	52.1	42.2	3.1	3.5	4.441	1943	0.81	8.6 ×10^6
HSNWC	68.2	58	4.7	5.6	5.487	2408	1.435	13.2 ×10^6

* For each mix, an average of three specimens was taken.

** λ: Thermal conductivity, this test was carried out at the national center for construction laboratories–Laboratory Baghdad.

*** AI: Acoustic Impedance = wc* UPV

3.2. General Cracking Behavior

The cracking performance of the tested slabs is evaluated and discussed as hereto: all tested slab specimens subjected to the effects of static two-point loading revealed three distinct stages of deformation. The deformations could be categorized as elastic deformations in the early stages of testing before the first crack was initiated. The crack appeared in the tension face of the tested slabs when the applied load reached the first cracking load, which ranged from 0.134 to 0.284 of the ultimate loads, as shown in Table 5. As the load increased, more flexural cracks started to appear at the tension face of the tested slab specimens and spread horizontally from the mid-span to the support. This stage represents the elastic-plastic stage. Then, cracks number along with cracks width increased and moved upwards to compression zone in one–way solid slab specimen and to the flange of the one–way ribbed slab specimens. Finally, a further increase in the load magnitude led to more reduction in the stiffness of the slab specimens (plastic stage) and then followed by failure. The failure of the slab specimen could be characterized as a flexural failure.

Figure 6. summarizes the cracking outlines of all specimens. From this figure, using HSLWC in producing one-way ribbed slab S1 instead of HSNWC in slab S2 decreased the number of cracks and increased their width due to the lower flexural rigidity of slab S1, which was due to the lower modulus of elasticity of HSLWC. Changing the steel reinforcement ratio (ρ) from 0.28% in slab S1 to 0.16% in slab S3 and 0.44% in slab S4 indicated that using a higher reinforcement ratio led to an increase in the number of cracks with the narrower widths. This behavior is due to an increase in the flexure rigidity of the ribbed slab. Changing the number of ribs from 3-ribs in HSLWC ribbed slab S1 to 2-ribs in slab S5 and 1-rib in slab S6 to study the effect of ribs geometry on cracking behavior indicated that the geometry of ribs had no significant effects on the cracking number and their widths at the same loading levels. This behavior may belong to the same amount of ribs reinforcement and concrete. Reducing the voiding ratio of HSLWC one-way ribbed slabs (S7 and S8) compared with slab S1 led to an increase in the number of narrower cracks width. This behavior was because of the enhancement in the moment of inertia and flexural rigidity of slabs. Producing a solid slab with the same HSLWC amount for ribbed slab negatively impacted the cracking behavior at the same load level due to a decrease in the thickness of the slab, which led to a decrease in the flexural rigidity of this slab. Moreover, the outcomes of the maximum crack widths from slab S1 to slab S9 at service load 0.65 of P_u [32] were (0.22, 0.11, 0.25, 0.18, 0.13, 0.10, 0.21, 0.17, and 0.12) mm, respectively, these results revealed that all slabs meet the crack widths limitation of ACI 318-19 [33] at service state which is 0.4 mm.

Table 5. Ultimate and cracking capacity for test specimens

Slab Symbol	P_{cr} (kN)	% Diff. in P_{cr}	P_u (kN)	% Diff. in P_u	$M_{n\,EXP.}$* (kN.m)	$M_{n\,ACI}$** (kN.m)	$M_{n\,EXP}/M_{n\,ACI}$
S1	12.51	---	77.15	---	23.15	18.05	1.28
S2	22.50	79.86	93.74	21.50	28.12	18.15	1.55
S3	11.54	-7.75	48.13	-37.62	14.44	10.05	1.44
S4	15.91	27.18	118.80	53.99	35.64	30.06	1.19
S5	12.86	2.80	77.45	0.39	23.24	18.05	1.29
S6	13.00	3.92	76.79	-0.47	23.04	18.05	1.28
S7	14.5	15.91	83.58	8.33	25.07	18.05	1.39
S8	16.78	34.13	88.70	14.97	26.61	18.05	1.47
S9	9.51	-23.98	33.49	-56.59	10.05	8.69	1.16
Mean							1.34
standard deviation (SD)							0.13
The coefficient of variation (COV) %							9.70

*$M_{nEXP.} = \frac{P_u}{2} * 0.6$

**$M_{n\,ACI} = \rho b\, d^2\, f_y\, (1 - 0.59\rho\, \frac{f_y}{f'_c})$

Figure 6. Cracking patterns for all tested slab specimens

The recorded test results of ultimate loads are given in Table 5, together with comparisons with values estimated with ACI code [33]. The coefficient of variation (COV), the standard deviation divided by the mean value of results, was 9.70%. The difference in estimated values of the ACI code may be because the ACI code assumed a uniaxial state of stresses in a one-way slab and neglected the effect of Poisson's ratio. Other reasons could be attributed that the ACI code eliminated the effects of concrete at the tension zone and friction between the (steel plate of supports and concrete), which leads to increasing the slab moment capacity.

3.3. Load–Deflection Curve

Load–deflection curves for all tested slab specimens, as shown in Figure 7.

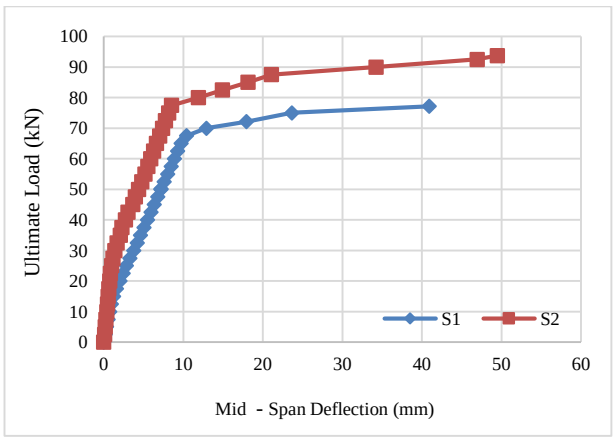

(a) Type of concrete effect

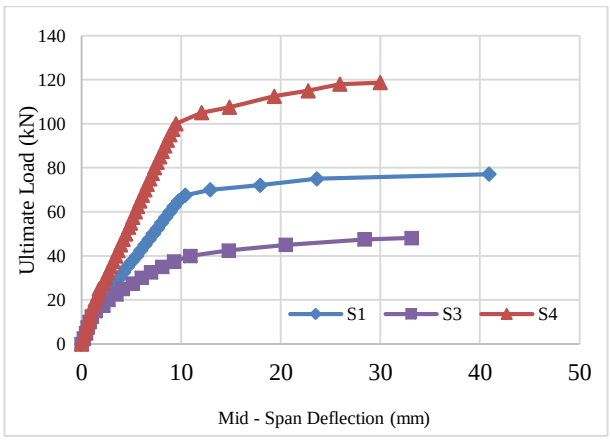

(b) Ratio of reinforcement effect

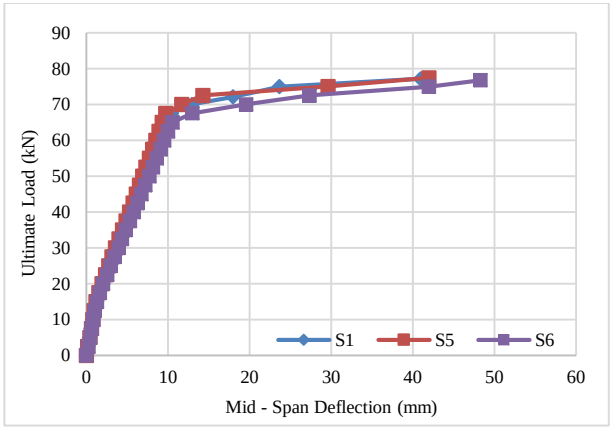

(c) Geometry of ribs effect

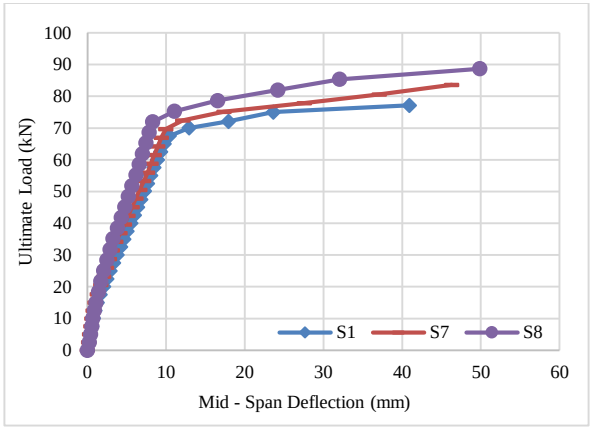

(d) Voiding ratio effect

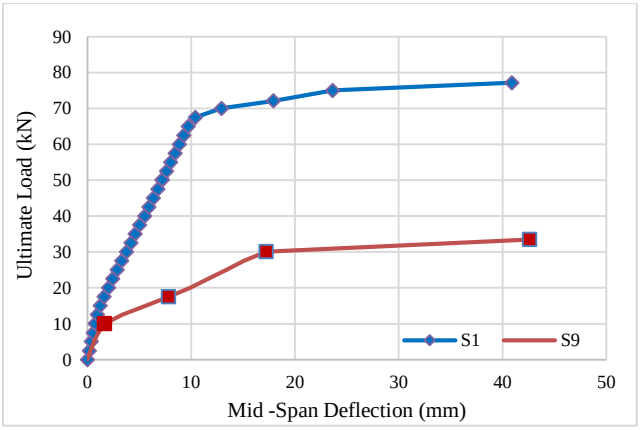

(e) Type of slab effect

Figure 7. Load–deflection curve for tested slab specimens

From this figure could be found that load-deflection response in all slabs appeared in three stages: elastic stage, elastic-plastic stage, and plastic stage behavior. Also, it was found that:

Using HSNWC in slab S2 instead of HSLWC increased the ultimate load capacity and ultimate deflection by 21.50 and 20.97%, respectively. In other words, using HSNWC in slab S2 gave a stiffer behavior than slab S1, as shown in Figure 7a. The main reason for this behavior was the use of LWA, thus leading to the weakening of the concrete. The same result was proved by [9]. Decreasing the ρ from 0.28 to 0.16% in slab S3 reduced the ultimate load and ultimate deflection by 37.62 and 19.04%, respectively. Increasing the ρ from 0.28 to 0.44% in slab S4 increased the ultimate load by 53.99% and decreased the ultimate deflection by 26.74%. Figure 7b indicates that the HSLWC one-way ribbed slabs with more ρ have a stiffer response. This tendency was primarily due to increasing the effective moment of inertia of the slab. The slabs S5 and S6 approximately gave similar values in ultimate strength capacity with a difference not exceeding 0.47%. While the ultimate deflection in slabs S5 and S6 increased by 2.54 and 17.94%, respectively, compared to slab S1. This behavior may belong to the stress distribution through the width of the slab (shear lag phenomena) due to the change of ribs number at the same concrete volume.

Reducing the voiding ratio from 44 to 40% in slab S7 and 33% in slab S8 gave increased the ultimate load-carrying capacity of slabs S7 and S8 by 8.33 % and 14.97 %, respectively. Furthermore, the ultimate deflection increased by 13.12 and 21.82%, respectively, the same deflection behavior result found in the previous study [1]. The reduction in the voiding ratio caused an improvement in the stiffness of slabs S7 and S8 compared to slab S1 at the same load level. This behavior appeared the significant role of the width of ribs in increasing the moment of inertia of slabs, thus the flexural rigidity improvement. Using HSLWC ribbed slab S1 instead of solid slab S9 increased the load-carrying capacity by 130.37 % and decreased the ultimate deflection by 3.99%. Figure 7e revealed a stiffer behavior of ribbed slab S1 compared to solid slab S9. This behavior belonged to the thickness of ribbed slab was higher than solid slab that led to increase in the section properties, thus the stiffness improvement.

3.4. Ductility Index

The displacement ductility index (μ_d) is defined as the ratio between the deflection at the maximum load and the deflection at the yielding load [34]. Yield load can be found in the (load-deflection curve) of the slab when the curve moves from the elasticity stage to the plasticity phase. Figure 8 shows the ductility index of tested slab specimens.

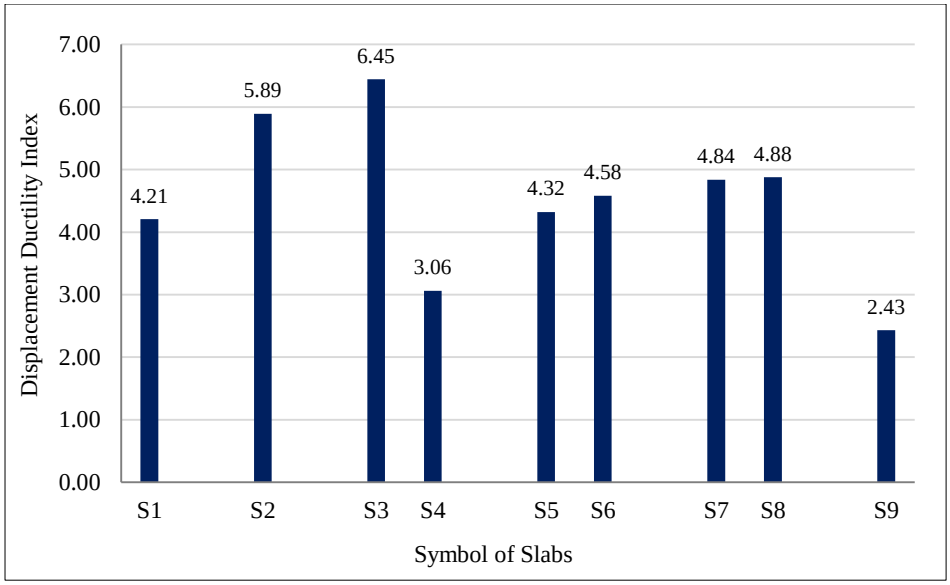

Figure 8. Ductility index of tested slab specimens

From Figure 8 can be found that:

Using HSNWC in slab S2 instead of HSLWC gave increasing in the μ_d by 39.90%, due to the nature of NWA having less brittleness than the LWA, the same response was found in previous studies [6, 9]. Decreasing of ρ from 0.28 to 0.16% in slab S3 led to an increase in the μ_d by 53.21%, while increasing the ρ from 0.28 to 0.44% in slab S4 led to a decrease in the μ_d by 27.32%. This behavior was because increasing the ρ improved the strength, which caused the yielding to be too far away to occur. Using different ribs geometry by changing the number of ribs from three to two ribs in S5 and one rib in S6 gave increasing in the μ_d by 2.61 % and 8.79 %, respectively. This behavior was due to the increase in the ultimate deformation. Decreasing the voiding ratio by increasing the width of rib from 120 mm in slab S7 and 150 mm in slab S8 in comparison to 100 mm in reference slab S1 gave increasing in the μ_d by 14.96 % and 15.91 %, respectively. This behavior was because of the effect of yield and ultimate deformations.

Converting the slab type from solid slab S9 to ribbed slab S1 led to an increase in the μ_d by 73.25 %. The μ_d of the solid slab was under lower limits of ductility requirement in seismic zones, which ranged from 3-5 [35]. This behavior was due to an increment in the yielding deformation.

3.5. Structural Efficiency

The strength/density ratio defines the structural efficiency (SE) [22]. In this study, the SE was calculated by dividing the ultimate strength by the total weight of the slab, as schematically depicted in Figure 9.

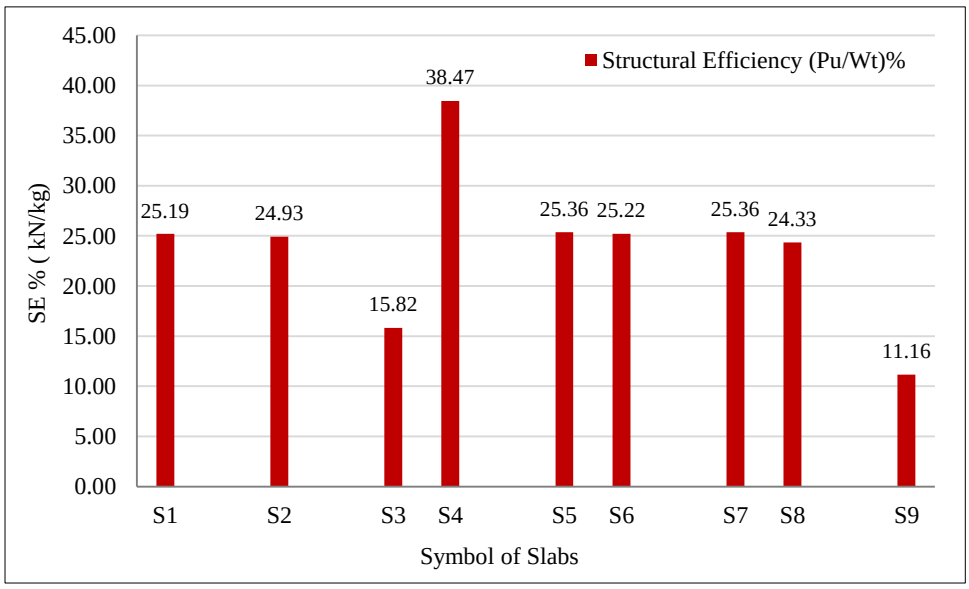

Figure 9. Structural efficiency of tested slab specimens

From Figure 9, the results of all the tested slabs can be illustrated as follows:

The SE of slab S1 has superiority over slab S2 despite slab S2 having higher strength. This behavior was due to the weight reduction of slab S1. Changing ρ from 0.28 to 0.16% in slab S3 decreased the SE by 37.2 % and to 0.44% in slab S4 increased the SE by 52.72 %, respectively. This behavior was due to the strength of slabs S3 and S4. Changing the number of ribs from three to two in slab S5 and one in slab S6 increased the SE by 0.67% and 0.12%, respectively. The SE of slabs S5 and S6 were nearly the same as slab S1. This behavior was due to the same weight of slab specimens, and the strength was very close to its values.

The SE in slab S7 increased by 0.67%, while it decreased in slab S8 by 3.41% compared to reference slab S1. This behavior was due to the strength and weight of these slabs; from these outcomes could be concluded that the slab S7 had an optimum voiding ratio. The SE of slab S1 has superiority on slab S9 by 125.72%. This behavior was due to the reduction of the strength of slab S9.

4. Conclusions

Through the experimental results of this study, it can be concluded that:

- Using pumice stone as coarse aggregate instead of gravel in the production of HSLWC led to an improvement in sustainability by decreasing the physical properties such as unit weight, thermal conductivity (i.e., an increase in thermal insulation), and sound impedance. However, this enhancement in physical properties was accompanied by a reduction in mechanical properties such as compressive and tensile strength.
- Using HSLWC in a ribbed slab instead of HSNWC led to a decrease in the ultimate load capacity by 17.70%. Overcoming the strength reduction was accomplished by increasing the steel reinforcement ratio from 0.28 to 0.44%.In addition, it has resulted in higher ultimate strength. However, this enhancement in strength was accompanied by a reduction in the ductility index.
- Changing the geometry sections of the HSLWC one-way ribbed slabs led to a significant improvement from an economic point of view, more than strength, due to reducing the number of fabrication shear reinforcements.
- Using HSLWC in the construction of solid slabs instead of ribbed slabs with the same amount of concrete gave a ductility index of less than 3.0. Hence, the solid slab needs more precautions, especially in seismic zones.
- Reducing the voiding ratio up to a certain limit improved the SE of the HSLWC ribbed slab.
- Using a one-way ribbed HSLWC slab instead of a one-way solid slab at the same concrete volume resulted in a 130.37% increase in ultimate load capacity and a 3.99% decrease in ultimate deflection.
- On the one hand, the ACI expression for the moment capacity of HSNWC becomes more conservative than the HSLWC ribbed slab; on the other hand, the ACI expression becomes less conservative as the steel ratio increases.

4.1. Recommendations and Future Direction

The authors recommend adding different types of fibers to the HSLWC mix to reinforce it and reduce the brittleness of LWA to obtain better benefits from using HSLWC in the production of one-way ribbed slabs. Furthermore, conducting a sustainability analysis concerning the impact of using HSLWC in producing one-way ribbed slabs. In the future, the authors suggest studying the same variables were adopted in this study under different ranges of high temperature to benefit from the volcanic nature of pumice stone and under different loading types such as dynamic loading

5. Declarations

5.1. Author Contributions

Conceptualization, T.A.M. and H.M.K.; methodology, T.A.M.; Investigation, T.A.M.; Writing—original draft preparation, T.A.M.; Writing—review and editing, T.A.M.; Supervision, H.M.K. All authors have read and agreed to the published version of the manuscript.

5.2. Data Availability Statement

The data presented in this study are available on request from the corresponding author.

5.3. Funding

The authors received no financial support for the research, authorship, and/or publication of this article.

5.4. Conflicts of Interest

The authors declare no conflict of interest

6. References

[1] Al-Azzawi, A. A., Abbas, J., & Al-Asdia. (2017). Behavior of one way reinforced concrete slabs with styropor blocks. Advances in Concrete Construction, 5(5), 451–468. doi:10.12989/acc.2017.5.5.451.

[2] Ashour, S. A. (2000). Effect of compressive strength and tensile reinforcement ratio on flexural behavior of high-strength concrete beams. Engineering structures, 22(5), 413-423. https://doi.org/10.1016/S0141-0296(98)00135-7.

[3] Hameed Naser Al-Mamoori, F., & Hameed Naser Al-Mamoori, A. (2018). Reduce the Influence of Horizontal and Vertical Cold Joints on the Behavior of High Strength Concrete Beam Casting in Hot Weather by Using Sugar Molasses. International Journal of Engineering & Technology, 7(4.19), 794. doi:10.14419/ijet.v7i4.19.27999.

[4] Altun, F., & Haktanir, T. (2001). Flexural Behavior of Composite Reinforced Concrete Elements. Journal of Materials in Civil Engineering, 13(4), 255–259. doi:10.1061/(asce)0899-1561(2001)13:4(255).

[5] Adil, M., & Abdulrazzaq, O. A. (2017). Flexural Behavior of Composite Reinforced Concrete Slabs. Iraqi Journal of Civil Engineering, 11(2), 55-65.

[6] Jomaa'h, M. M., Ahmed, S., & Algburi, H. M. (2018). Flexural Behavior of Reinforced Concrete One-Way Slabs with Different Ratios of Lightweight Coarse Aggregate. Tikrit Journal of Engineering Sciences, 25(4), 36–44. doi:10.25130/tjes.25.4.07.

[7] Adheem, A. H., Rasheed, L., & Ali, I. M. (2018). Flexural behavior of lightweight aggregate concrete one-way slabs. International Journal of Civil Engineering and Technology, 9(13), 277–289.

[8] Selwyn Babu, J., & Rex, J. (2019). Experimental investigation on lightweight concrete slabs. International Journal of Recent Technology and Engineering, 7(5), 502–506.

[9] Khalil, Ali Omer. (2018). Behavior of Light Weight Aggregate Concrete Slabs with Styropor Blocks. MSc. Thesis, Al-Nahrain University, Baghdad.

[10] Al-Nasra, M., Abdulraziq, R., Abouelnaga, Y., AlMofleh, A., Ayub, O., Abdelsadig, M., & Mohammed, O. (2019). Investigating the Effect of the Ribs Spacing on the One Way Reinforced Concrete Ribbed Slab Strength. Journal of Engineering and Applied Sciences, 14(15), 5138–5142. doi:10.36478/jeasci.2019.5138.5142.

[11] Buka-Vaivade, K., Sliseris, J., Serdjuks, D., Sahmenko, G., & Pakrastins, L. (2019). Numerical Comparison of HPFRC and HPC Ribbed Slabs. IOP Conference Series: Materials Science and Engineering, 660(1), 12054. doi:10.1088/1757-899X/660/1/012054.

[12] Huang, W., Ma, X., Luo, B., Li, Z., & Sun, Y. (2019). Experimental Study on Flexural Behaviour of Lightweight Multi-Ribbed Composite Slabs. Advances in Civil Engineering, 2019, 1–11. doi:10.1155/2019/1093074.

[13] Liu, J., Hu, H., Li, J., Chen, Y. F., & Zhang, L. (2020). Flexural behavior of prestressed concrete composite slab with precast inverted T-shaped ribbed panels. Engineering Structures, 215(110687). doi:10.1016/j.engstruct.2020.110687.

[14] S. Abdulhussein, S., & A. Alfeehan, A. (2020). Experimental Study of Depth Variation in Flanged Ribbed Lightweight Concrete Slabs. Journal of Engineering and Sustainable Development, 24(Special), 359–364. doi:10.31272/jeasd.conf.1.38.

[15] Buka-Vaivade, K., Serdjuks, D., Sliseris, J., Podkoritovs, A., & Ozolins, R. (2021). Timber-concrete composite ribbed slabs with high-performance fibre-concrete. Vide. Tehnologija. Resursi - Environment, Technology, Resources, 3, 40–44. doi:10.17770/etr2021vol3.6551.

[16] European Committee for Standardization. (2011). Cement: Composition, Specifications and Conformity Criteria for Common Cements. British Standards Institute, London, UK.

[17] ASTM C1240-15. (2020). C1240 Standard Specification for Silica Fume Used in Cementitious Mixtures. In Annual Book of ASTM Standards. American Society for Testing and Materials, P.A., United States.

[18] Iraqi Specification Standard No.45/1984. (1984). Aggregate of natural sources using in concrete and building. Central Organization for Standardization and Quality Control, Baghdad, Iraq.

[19] ASTM C330/C330M-17a. (2017). Standard Specification for Lightweight Aggregates for Structural Concrete. American Society for Testing and Materials, P.A., United States.

[20] ASTM C 494-19. (2019). Standard Specification for Chemical Admixtures for Concrete. American Society for Testing and Materials, P.A., United States.

[21] ASTM A615 Specification for Deformed and Plain Carbon-Steel Bars for Concrete Reinforcement. (2020). American Society for Testing and Materials, P.A., United States.

[22] ACI 213R-14. (2014). Guide for Structural Lightweight Concrete. American Concrete Institute, Indiana, United States.

[23] ACI 363R-10. (2010). Report on High-Strength Concrete. American Concrete Institute, Indiana, United States.

[24] BS 1881-Part 116. (2000). Method for Determination of Compressive Strength of Concrete Cubes. British Standards Institute, London, UK.

[25] ASTM C39/C39M − 15a. (2015). Standard Test Method for Compressive Strength of Cylindrical Concrete Specimens. American Society for Testing and Materials, P.A., United States.

[26] ASTM C496/C496M−17. (2017). Standard Test Method for Splitting Tensile Strength of Cylindrical Concrete Specimens. American Society for Testing and Materials, P.A., United States.

[27] ASTM C78/C78M−18. (2018). Standard Test Method for Flexural Strength of Concrete (Using Simple Beam with Third-Point Loading). American Society for Testing and Materials, P.A., United States.

[28] ASTM C597. (2016). Standard Test Method for Pulse Velocity through Concrete. In American Society for Testing and Materials, West Conshohocken, PA, USA. American Society for Testing and Materials, P.A., United States.

[29] ASTM C567/C567M−19. (2019). Standard Test Method for Determining Density of Structural Lightweight Concrete. American Society for Testing and Materials, P.A., United States.

[30] ASTM C642-13. (2013). Standard Test Method for Specific Gravity, Absorption, and Voids in Hardened Concrete. In ASTM International, West Conshohocken, American Society for Testing and Materials, P.A., United States.

[31] ASTM C-1113 (2009) Standard Test Method for Thermal Conductivity of Refractories by Hot Wire (Platinum Resistance Thermometer Technique). American Society for Testing and Materials. Reapproved 2013, P.A., United States.

[32] Jeffrey, S. R. (2003). Prestrectives in civil engineering. Commemorating the 150th anniversary of the American Society of Civil Engineering, United States.

[33] ACI Commentary 318-19. (2019). Building Code Requirements for Structural Concrete. American Concrete Institute, Indiana, United States.

[34] Hao, Y., Hao, H., & Chen, G. (2014). Experimental investigation of the behaviour of spiral steel fibre reinforced concrete beams subjected to drop-weight impact loads. Materials and Structures, 49(1-2), 353–370. doi:10.1617/s11527-014-0502-5.

[35] Ahmad, S. H., & Barker, R. (1991). Flexural behavior of reinforced high-strength lightweight concrete beams. ACI Structural Journal, 88(1), 69–77. doi:10.14359/2753.